Supplemental File S1

World Scientists' Warning of a Climate Emergency 2022

By William J. Ripple, Christopher Wolf, Jillian W. Gregg, Kelly Levin, Johan Rockström, Thomas M. Newsome, Matthew G. Betts, Saleemul Huq, Beverly E. Law, Luke Kemp, Peter Kalmus, and Timothy M. Lenton

Table of Contents

Supplemental Tables

Table S1. Summary of variables shown in Figures 2 and 3. Table columns show the variable name, update frequency, number of years with data, time of most recent data point, current value of the variable, change relative to the previous value, and rank (where rank 1 indicates the highest value to date). For variables with subannual frequency, the value, change, and rank are all based on year-to-date data. For example, they are based on the first 20.8% of each year for the variable "Carbon dioxide (CO_2 parts per million)" (since "Year" is equal to 2021.208). Note that variable time spans (# of years) differ significantly depending on the source. Variables that set all-time records based on the time series data are shown in red and marked with asterisks. Sources for these variables are given in this supplement.

Variable	Type	Years	Year	Value	Change	Rank
Human population (billion individuals)*	Annual	73	2022	7.95	0.079	1
Total fertility rate (births per woman)*	Annual	61	2020	2.39	-0.0146	61
Ruminant livestock (billion individuals)*	Annual	60	2020	4.12	0.0579	1
Per capita meat production (kg/yr)	Annual	60	2020	43.3	-0.233	8
World GDP (trillion current US $/yr)*	Annual	63	2022	89.8	3.11	1
Global tree cover loss (million hectares/yr)	Annual	21	2021	25.3	-0.53	4
Brazilian Amazon forest loss (million hectares/yr)	Annual	34	2021	1.32	0.215	18
Coal consumption (Exajoules/yr)	Annual	57	2021	160	9.03	3
Oil consumption (Exajoules/yr)	Annual	57	2021	184	10	5
Gas consumption (Exajoules/yr)*	Annual	57	2021	145	6.91	1
Solar/wind consumption (Exajoules/yr)*	Annual	57	2021	27.3	4.17	1

Air transport (billion passengers carried/yr)	Annual	48	2020	1.81	-2.75	17
Total institutional assets divested (trillion USD)*	Annual	11	2022	39.2	24.5	1
CO_2 emissions (gigatonnes CO_2 equivalent/yr)	Annual	32	2021	39	2.01	3
Per capita CO_2 emissions (tonnes CO_2 equivalent/yr)	Annual	32	2021	4.95	0.207	14
GHG emissions covered by carbon pricing (%)*	Annual	33	2022	23.1	0.09	1
Carbon price ($ per tonne CO_2 emissions)	Annual	33	2022	14.2	0.0933	22
Fossil fuel subsidies (billion USD/yr)	Annual	12	2021	440	259	7
Governments that have declared a climate emergency (#)*	Annual	6	2021	2080	146	1
Carbon dioxide (CO_2 parts per million)*	Subannual	43	2022.375	418	2.48	1
Methane (CH_4 parts per billion)*	Subannual	39	2022.292	1910	19.7	1
Nitrous oxide (N_2O parts per billion)*	Subannual	45	2022.286	336	1.46	1
Surface temperature anomaly (change) (°C)	Subannual	143	2022.537	0.903	0.101	5
Minimum Arctic sea ice (million km^2)	Annual	43	2021	4.92	0.92	32
Greenland ice mass change (gigatonnes)*	Subannual	21	2022.45	-5090	-198	21
Antarctica ice mass change (gigatonnes)	Subannual	21	2022.45	-2460	199	19

Glacier thickness change (m of water equivalent)*	Annual	72	2021	-25.5	-0.771	72
Ocean heat content change (10^{22} joules)*	Annual	17	2021	27.2	1.64	1
Ocean acidity (pH)	Subannual	33	2020.964	8.07	0.00994	24
Sea level change relative to 20-year mean (mm)*	Subannual	30	2022.413	53.1	2.82	1
Area burned in the United States (million hectares/yr)	Annual	39	2021	2.88	-1.21	13
Global tree cover loss due to fires (million hectares/yr)	Annual	21	2021	9.3	0.451	2
Billion-dollar floods in the United States (events/year)	Annual	42	2021	2	2	10
Extremely hot days relative to 1961-1990 (% of days/year)	Annual	71	2021	19	-0.47	2
Dengue virus vector capacity (average % change ca. 1950)	Annual	68	2017	11.2	-0.262	2

Table S2. Regional summaries for 24 countries and The European Union. Variables shown are "CO2" (total CO2 emissions associated with fossil fuel consumption in mega tonnes CO2), "Population" (human population size in millions), "CO2/capita" (CO2 emissions per capita in tonnes per person), "Share" (percentage of all CO2 emissions associated with fossil fuel consumption compared to the global total), and "GDP/capita" (per capita gross domestic product in US dollars per person). All data are for the year 2020 except GDP for Japan and the United Arab Emirates, which are for 2019. Additional details on these variables are provided in the supplementary information below. GDP/capita was calculated using FAOSTAT population estimates and World Bank GDP estimates.

	CO_2	Population	CO_2/capita	Share	GDP/capita
China	12040	1476	8.2	30.9%	$10,704
United States	5168	333	15.5	13.3%	$61,092
The European Union	3060	514	6.0	7.9%	$34,568
India	2797	1393	2.0	7.2%	$1,961
Russia	2172	146	14.9	5.6%	$10,218
Japan	1082	126	8.6	2.8%	$35,175
Iran	893	85	10.5	2.3%	$5,268
Indonesia	713	276	2.6	1.8%	$3,856
Saudi Arabia	679	35	19.2	1.7%	$19,018
South Korea	629	51	12.3	1.6%	$32,924
Canada	595	38	15.6	1.5%	$44,151
Brazil	496	214	2.3	1.3%	$8,551
South Africa	473	60	7.9	1.2%	$5,865
Turkey	448	85	5.3	1.1%	$13,251
Mexico	444	130	3.4	1.1%	$9,255
Australia	433	26	16.8	1.1%	$58,669
Vietnam	340	98	3.5	0.9%	$3,373
Thailand	302	70	4.3	0.8%	$6,270
UAE	293	10	29.3	0.8%	$37,120
Iraq	290	41	7.0	0.7%	$4,466
Kazakhstan	272	19	14.3	0.7%	$11,269
Egypt	267	104	2.6	0.7%	$4,086

Malaysia	267	33	8.1	0.7%	$10,827
Pakistan	258	225	1.1	0.7%	$1,507
Algeria	245	45	5.5	0.6%	$3,914
Top 25	**34656**	**5634**	**6.2**	**88.9%**	**$13,660**
World	**38977**	**7875**	**4.9**	**100.0%**	**$11,004**

Supplemental Figures

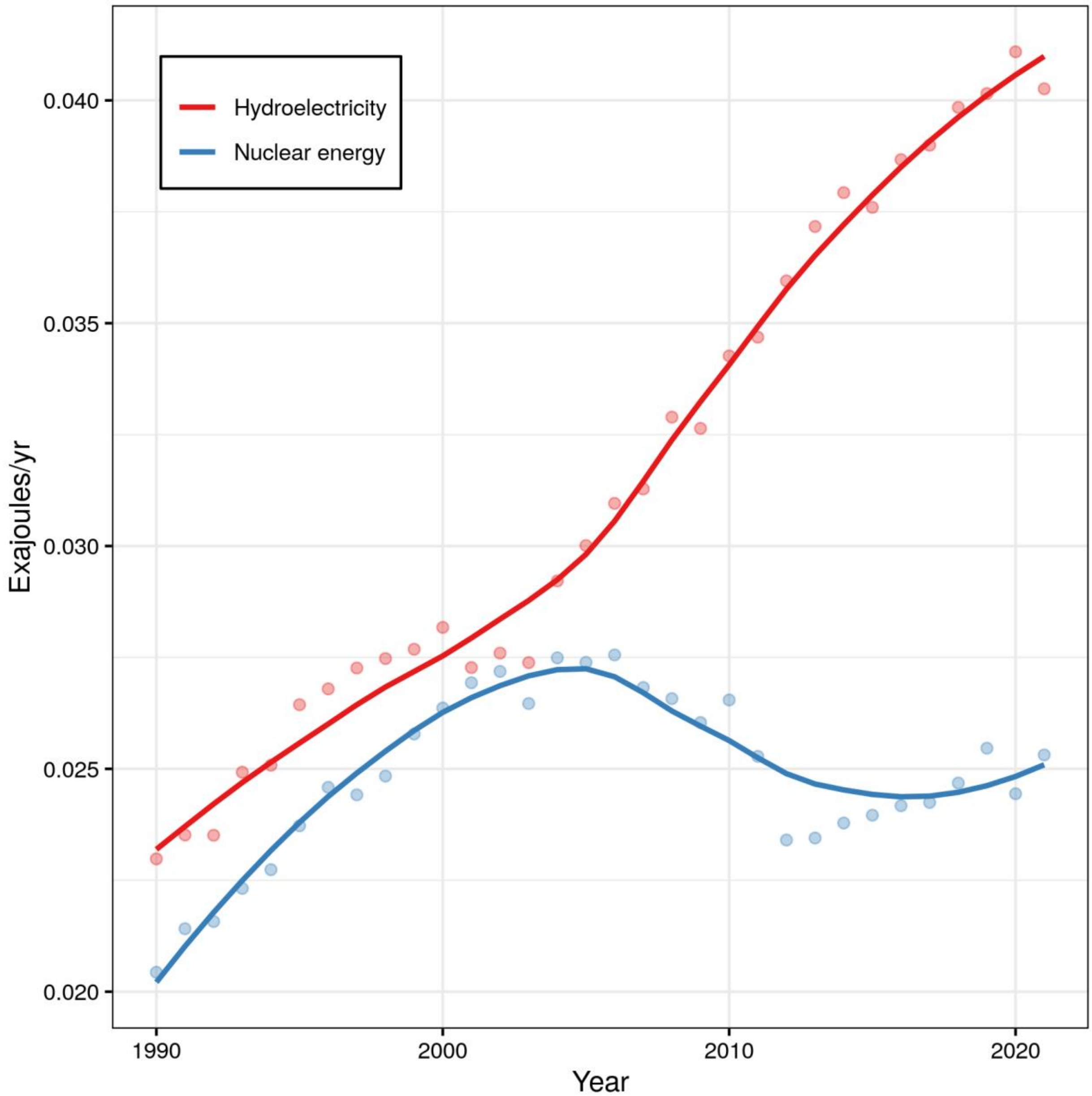

Figure S1. Annual consumption rates for nuclear energy and hydroelectricity (British Petroleum Company 2022). Non-fossil fuel energy supply pathways in the future may include hydro and nuclear power in addition to wind and solar power (IPCC 2018). See British Petroleum Company (2022) for other minor energy sources not shown in this figure. Figure 2h in the main text shows consumption of fossil fuels as well as solar/wind energy.

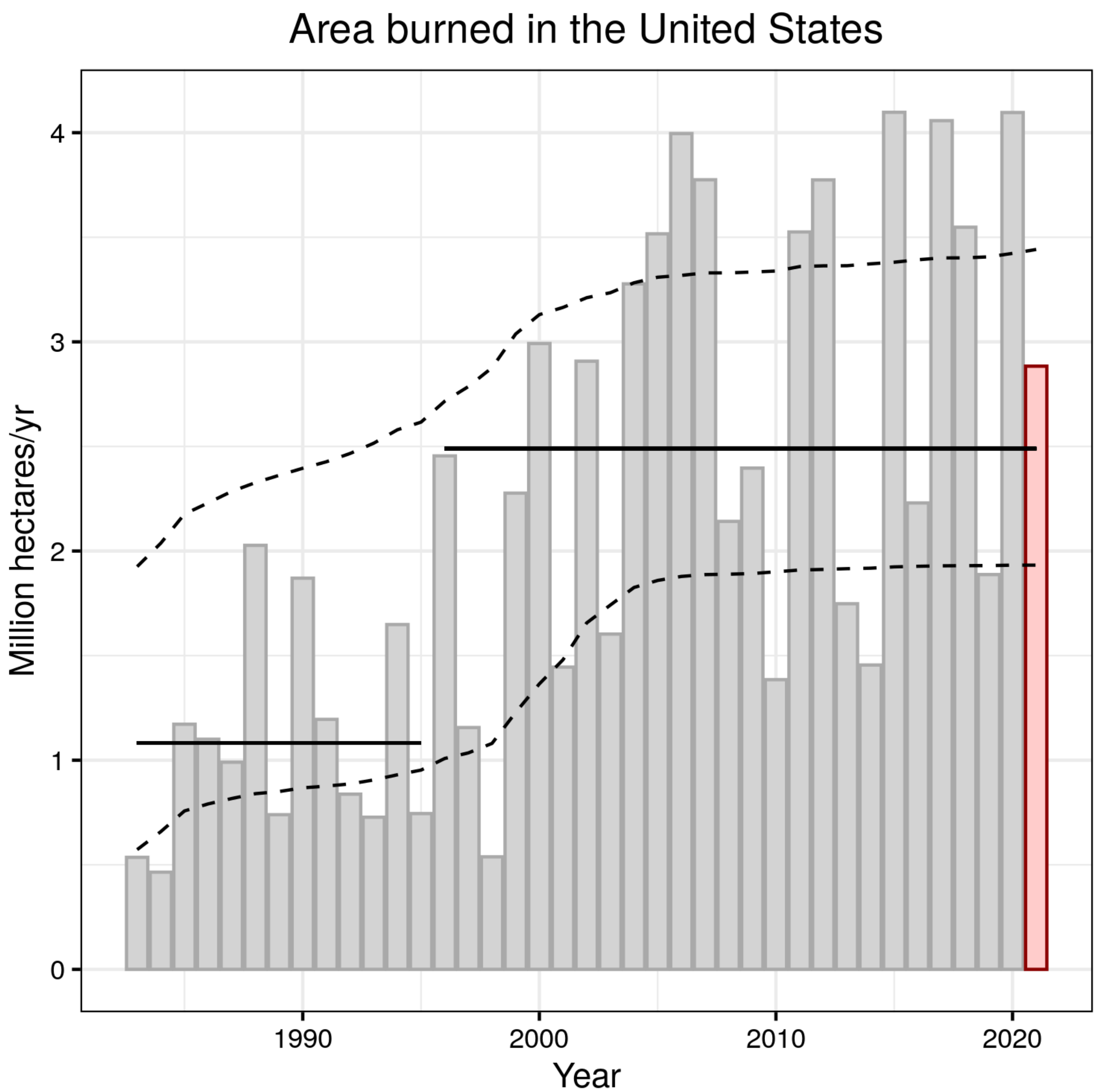

Figure S2. Approximate area burned in the U.S. (see figure 3l). The solid black lines show the predicted mean area burned according to a Bayesian change-point regression model. The dashed black lines correspond to an 80% credible band. According to this model, a new fire regime began around 1996 [80% credible interval: (1985, 2004)], although more research is needed to support this finding. Weakly informative priors were used for the rate parameters and inference was based on 4,000 posterior samples (see Supplementary Methods).

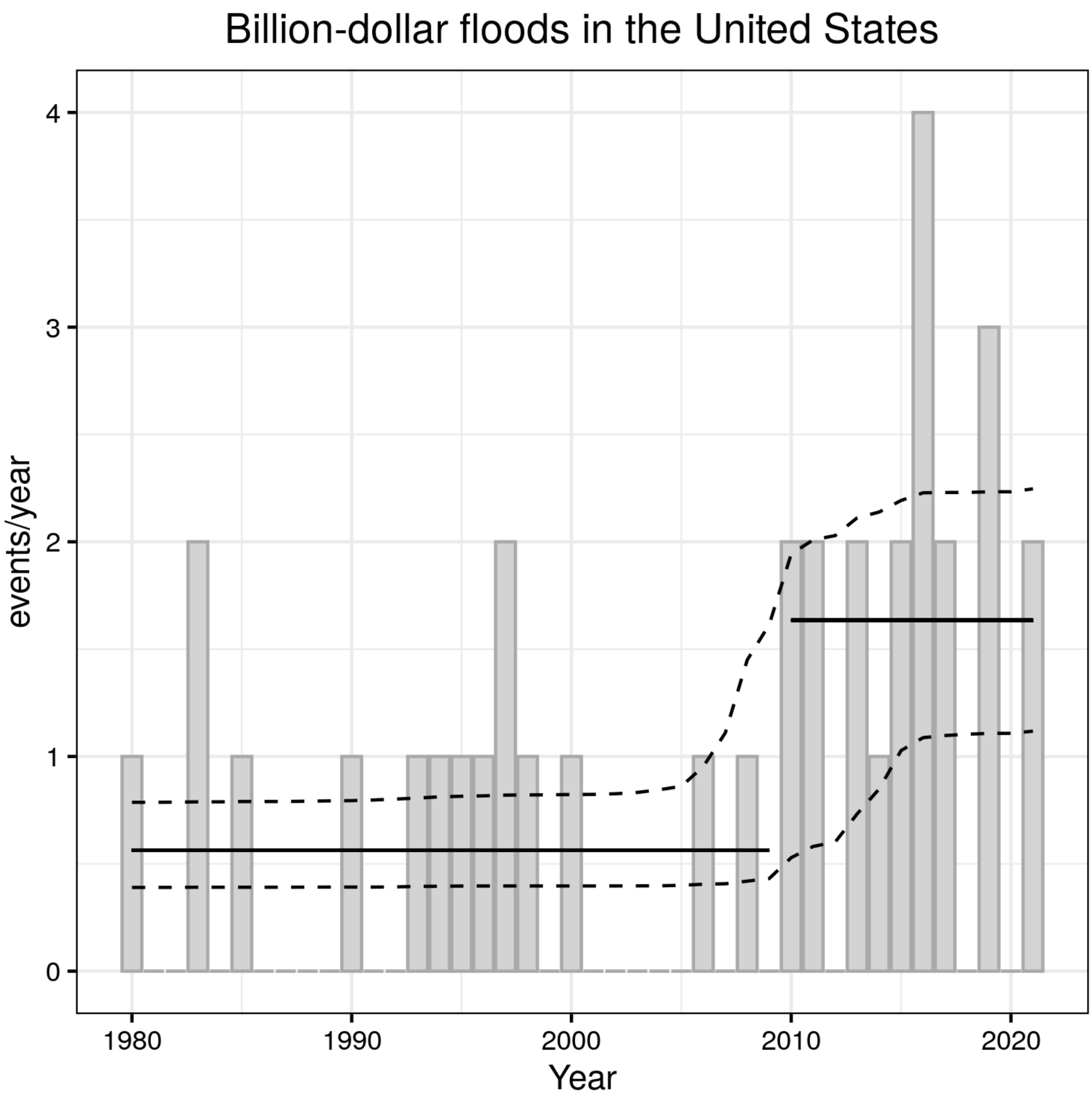

Figure S3. Number of inflation-adjusted billion-dollar floods in the U.S. (see figure 3n). The solid black lines show the predicted mean number of floods according to a Bayesian change-point regression model. The dashed black lines correspond to an 80% credible band. According to this model, a new flood regime began around 2010 [80% credible interval: (2006, 2014)], although more research is needed to support this finding. Weakly informative priors were used for the rate parameters and inference was based on 4,000 posterior samples (see Supplementary Methods).

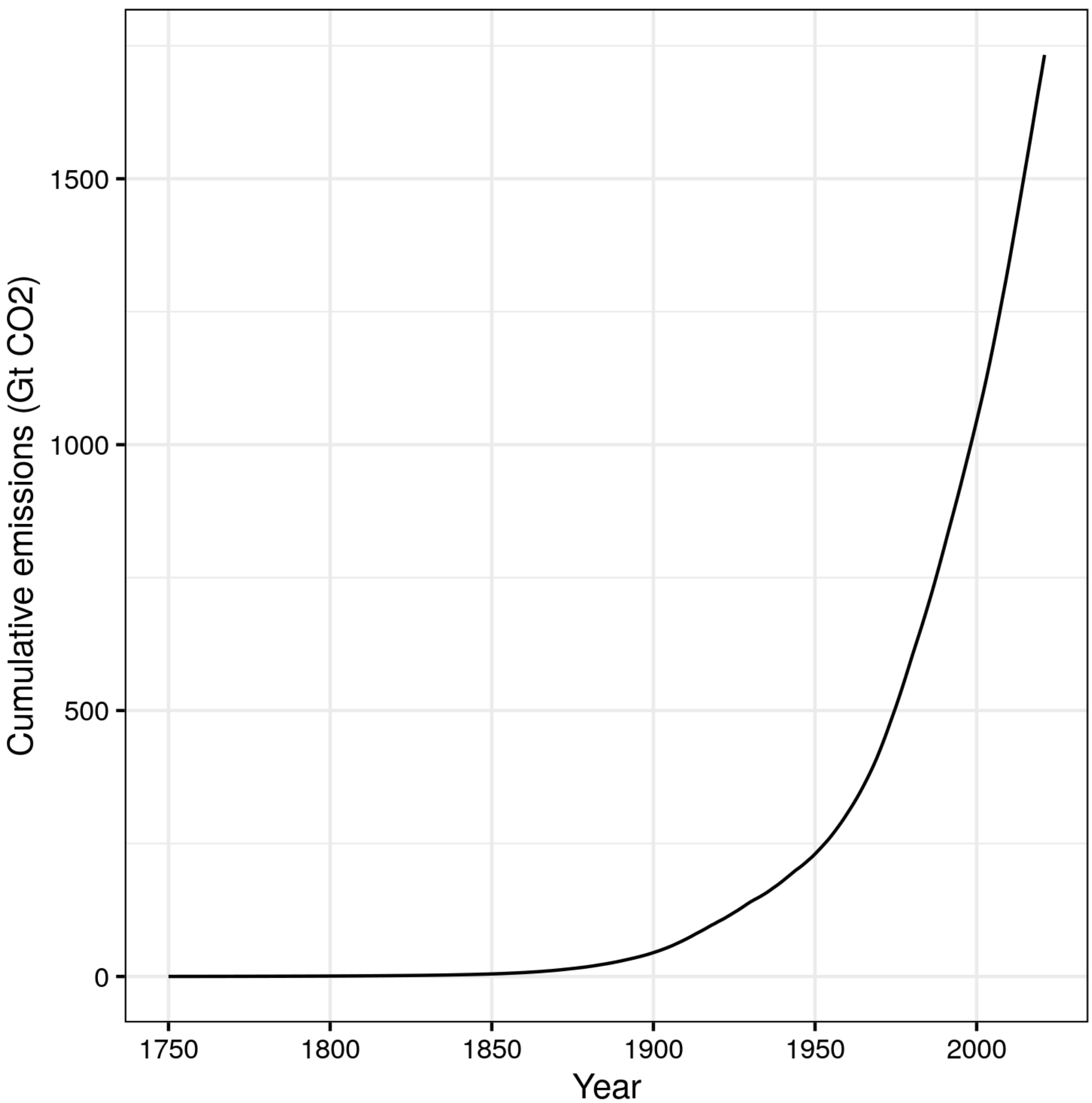

Figure S4. Cumulative fossil CO_2 emissions (excluding carbonation) relative to 1750. Data from 1750-2020 are from Friedlingstein et al. (2022), and the 2021 estimate is from Hausfather (2022). Addressing the climate emergency will require detailing with the massive building of carbon dioxide in the atmosphere. Otherwise, elevated CO2 levels and global temperatures, and could persist for centuries. An emissions counter developed using these data can be viewed at https://wolfkind.neocities.org/CO2/counter.html.

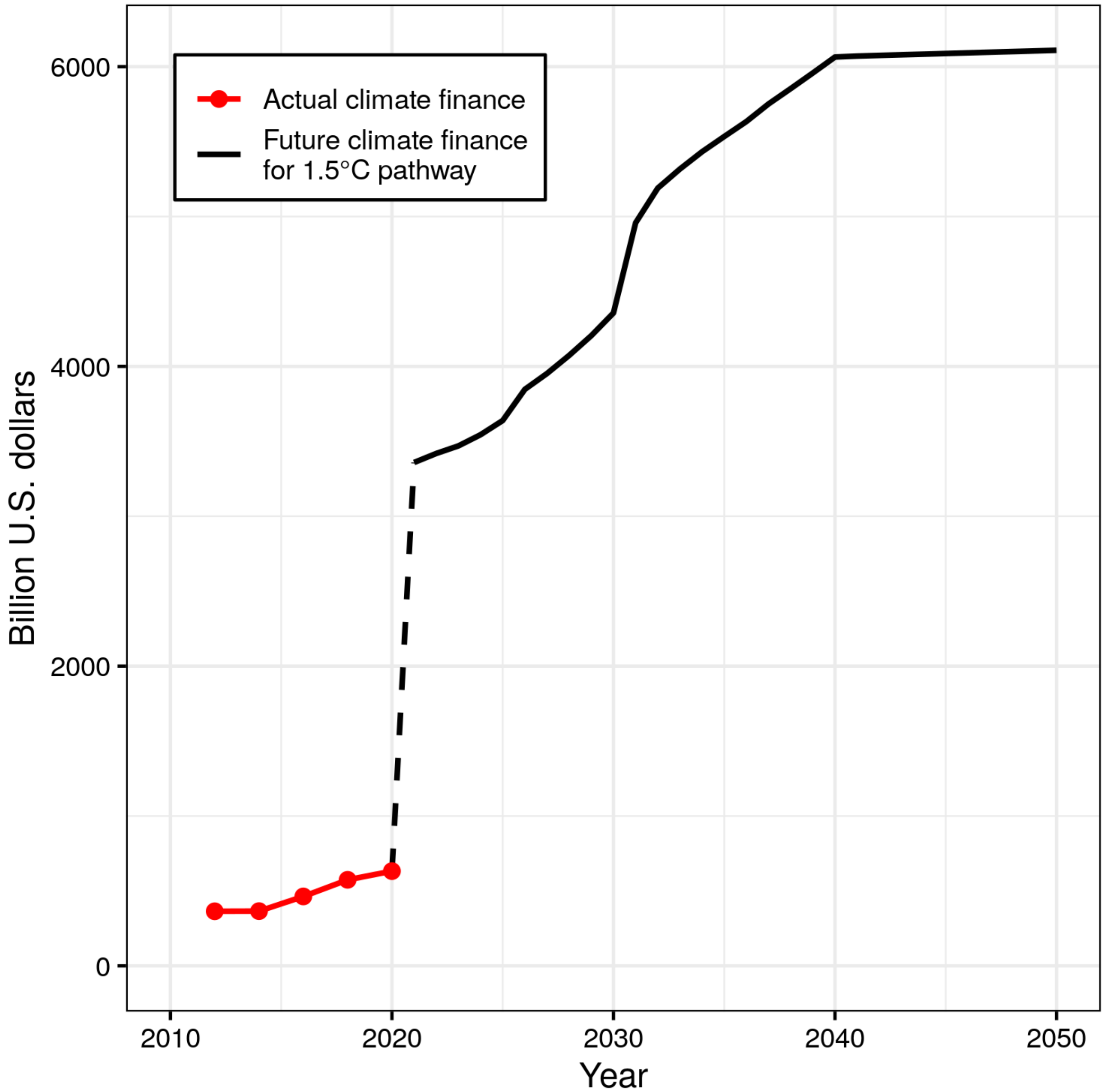

Figure S5. Global historical and needed climate finance/investment. The red line shows actual climate finance from 2012 to 2020. The black line shows needed climate finance (2021-2050) in order to follow the 1.5°C pathway. This figure is adapted from a similar version presented in the Climate Policy Initiative's "Global Landscape of Climate Finance 2021" report (Buchner et al. 2021). For additional details on these data, see Buchner et al. (2021).

Recent climate-related disasters (Table 1)

Below, we list a range of recent disasters from 2022 that were at least partly related to climate change. This list is not intended to be exhaustive. Due to the recent nature of these events, our sources often include news media articles. This list is identical to the one in Table 1 except relevant news articles and reports are provided using hyperlinks.

Because of the natural variability and stochasticity of the Earth system, attributing specific extreme events (or parts of their impacts) to climate change is an exceptionally challenging task (Stott et al. 2013, Trenberth et al. 2015), although it may be possible in some cases (e.g., Strauss et al. 2021). For simplicity, we have partly adopted the framework of Stott et al. (2013), which is described by Trenberth et al. (2015 p. 725) as follows:

"[T]he approach is to characterize the event and ask (i) whether the likelihood or strength of such events has changed in the observational record, and (ii) whether this change is consistent with the anthropogenic influence as found in one or more climate models, and thereby assess the 'fraction of attributable risk'."

For each event, we provide one or more references indicating that climate change may have increased the likelihood or intensity of such events. However, the references generally do not report the "fraction of attributable risk" as these analyses are often not yet available.

Note that some of these climate disasters may be at least partly related to changes in jet streams (Stendel et al. 2021, Rousi et al. 2022).

- (January-September, 2022) Many rivers in Europe have run low or dried up partly because of the worst drought in 500 years and intense heat waves. Climate change has likely played a significant role in this crisis by increasing the frequency and intensity of droughts and heat waves.
- (February, 2022) La Niña and climate change contributed to record-breaking rainfall on the east coast of Australia. This led to flooding that damaged thousands of properties and killed eight people.
- (February-March, 2022) Record-breaking flooding occurred along the northeastern coast of Australia, leading to standing water, which in turn promoted the spread of mosquitoes that carry the Japanese encephalitis virus. Such flooding is likely becoming more common due to climate change.
- (February-July, 2022) The number of people affected by drought in Kenya, Somalia, and Ethiopia who have limited access to safe water increased from 9.5 million to 16.2 million. This increasing drought severity may be at least partly due to climate change (Ghebrezgabher et al. 2016).

- (March, 2022) A severe drought in the Southern U.S. Plains put the winter wheat crop at risk. Although droughts are complex phenomena with many possible causes, increasing drought intensity has been linked to climate change (Mukherjee et al. 2018).
- (March-April, 2022) A deadly heat wave occurred in India and Pakistan, killing at least 90 people and contributing to widespread crop losses and wildfires. It was estimated that climate change made this event 30 times more likely to occur.
- (April, 2022) Climate change likely contributed to extreme rainfall in Eastern South Africa, which triggered flooding and landslides that killed at least 435 people and affected more than 40,000 people.
- (April-June, 2022) Widespread dust storms in the Middle East led to thousands of people being hospitalized; such dust storms may be increasing in frequency due to climate change.
- (May, 2022) Extremely heavy rainfall in northeastern Brazil resulted in landslides and flooding that killed at least 100 people. Climate change may be responsible for the increasing frequency of extreme rainfall.
- (June, 2022) A severe storm in Yellowstone (United States) caused the Gardner River to overflow, destroying parts of the road at Yellowstone National Park's north entrance. Such extreme flooding could be increasing in frequency due to climate change.
- (June, 2022) Several countries in Western Europe experienced a record-breaking heat wave. This heat wave contributed to major wildfires in Spain and Germany. Many other parts of the Northern Hemisphere also experienced extreme heat; for example, temperatures reached 104.4 F in Isesaki, Japan—an all-time record for the country. Similarly, a heat dome in the United States contributed to record-breaking temperatures. Other affected countries include Finland, Iran, Norway, and Italy. In general, extreme heat is becoming more common due to climate change (Luber and McGeehin 2008).
- (June, 2022) Following extreme heat, China experienced record-breaking rainfall, which may be linked to climate change.
- (June, 2022) Bangladesh experienced the worst monsoon flooding in 100 years, killing at least 26 people. This flooding is likely at least partly due to climate change causing monsoons to become more variable.
- (June-July, 2022) Extreme rainfall led to flooding in some parts of New South Wales, Australia. Sydney is currently on track to experience the wettest year on record. It is likely that climate change contributed at least partly to this rainfall and flooding.
- (June-August, 2022) Deadly floods in Pakistan have killed more than 1,000 people and affected roughly 33 million people, including 16 million children, since mid-June. Impacts include surging rates of dengue fever, gastric infections, and malaria. These floods may be partly related to climate change causing monsoon rainfall to become more intense.

- (June-August, 2022) China experienced an extraordinary heat wave, which may be the most severe that has ever been recorded globally. Such events are likely becoming more common because of climate change. The extreme heat contributed to large-scale crop failures and wildfires, in addition to exacerbating a major drought that caused 66 rivers to dry up and led to a significant decline in hydroelectricity generation.
- (August-September, 2022) California and other parts of the Western United States faced extremely hot temperatures due to a heat dome, which caused seven firefighters to be hospitalized with heat-related injuries. The effects of the heat dome may have been worsened by climate change.
- (September-October, 2022) In the United States, Hurricane Ian caused damage across many parts of Florida and the Carolinas, killing more than 100 people and leaving at least 2.5 million without electrical power. Ian is one of the costliest and strongest hurricanes to ever hit the United States. Climate change is likely causing strong and rapidly intensifying storms such as Ian to become more common.

Climate Impacts: Untold Human Suffering in Pictures

Here, we present a compilation of photographs intended as a visual demonstration of the recent impacts of climate change. Photos generally show human suffering due to natural disasters that may be at least partly attributable to climate change. The photos primarily come from the last decade (2013-2022) and are grouped into two themes: flooding and drought.

All photos are Creative Commons licensed and most were obtained through the Climate Visuals project (https://climatevisuals.org/), which compiles images from many sources. Specific credits are given with each image along with a brief description of the event. All quotations describing images are from the Climate Visuals project.

Part I. Flooding

South Sudan, 2014. “Two small boys wading through water in a rural landscape, a flood plain.”
Credit: JC Mcllwaine / UNMISS, Creative Commons

Bangladesh, 2020. Houses are nearly submerged due to flooding in Sirajganj, Bangladesh.
Credit: Moniruzzaman Sazal / Climate Visuals Countdown, Creative Commons

United Kingdom, 2007. “Torrential rainfall in South Yorkshire on the 25th June 2007 led to the beck flooding in the afternoon.” Credit: John Dal, Creative Commons

Uganda, 2020. “A girl, duck in hand wades through the water in Rwangara where Lake Albert levels caused the area to flood, destroying countless homes.” Credit: Climate Centre, Creative Commons

United Kingdom, 2014. “Man wades through flooded Cornish high street in the village of Fowey.” Credit: Prawny / Pixabay, Creative Commons

Mozambique, 2019. “Two young people carrying large electrical goods through flood waters, amplifiers.”
Credit: Denis Onyodi / IFRC/DRK, Creative Commons

Bangladesh, 2018. “Surviving against climate tragedy, two children a girl and a boy on a flooded riverbank.” Credit: Moniruzzaman Sazal / Climate Visuals Countdown

United Kingdom, 2008. “Residents wade through flooded streets to escape flood waters”
Credit: John Dal, Creative Commons

Part II. Drought

Afghanistan, 2019. “In the Afghan city of Bamiyan, young girls are caught by a sandstorm on their way to school.” Credit: Solmaz Daryani / Climate Visuals Countdown, Creative Commons


Kenya, 2017. “Drought in Kenya's Ewaso Ngiro river basin, transporting water by donkey cart.”
Credit: Denis Onyodi / Denis Onyodi/KRCS, Creative Commons


United States, 2012. Drought-affected corn field in Paulding County, Ohio.
Credit: U.S. Department of Agriculture / Christina Reed, Creative Commons.

Ethiopia, 2016. "Children in dust storm."
Credit: Anouk Delafortrie / EU/ECHO, Creative Commons

Kenya, 2017. "Pastoralists living in the Ewaso Ngiro river basin in central Kenya are digging for water and fear they will have to begin large-scale cattle destocking if the next rains are poor."
Credit: Denis Onyodi / KRCS, Creative Commons

United States, 2012. Agriculture Secretary Tom Vilsack examines crop damage due to a drought in Iowa.
Credit: U.S. Department of Agriculture / Darin Leach


Mozambique, 2016. A water hole that may have become empty due to drought.
Credit: Aurélie Marrier d'Unienville / IFRC

Climate feedback loops and tipping points

Rising global temperatures increase the risks posed by feedback loops and tipping points (Lenton et al. 2019). For example, climate change and deforestation have together pushed the Amazon rainforest beyond critical thresholds, raising concerns about multiple positive feedback loops in this important ecosystem (Boulton et al. 2022). Likewise, warming in the Arctic can cause accelerated release of greenhouse gasses from permafrost, potentially leading to further warming (Schuur et al. 2015).

Planetary boundaries

The climate crisis cannot be addressed as a stand alone issue. It is part of a larger systemic problem; a manifestation of the fact that humanity is now deep into the Anthropocene, where human demand exceeds the regenerative capacity of the biosphere (Wackernagel et al. 2002) and where Earth is losing its resilience to deal with stress and disturbance. The latest assessments indicate that 6 of the 9 planetary boundaries that contribute to regulate the state of the planet are beyond their safe space (Steffen et al. 2015, Persson et al. 2022, Wang-Erlandsson et al. 2022) (Steffen et al., 2015; Persson et al., 2022; Lan-Erlandsson et al., 2022), and that protecting nature (land, biodiversity, freshwater, nutrients) can help determine whether or not we are able to hold the agreed Paris climate target of 1.5°C (Rockström et al. 2021). A safe landing on climate requires massive action on both tackling ecological overshoot and decarbonising the global energy system.

Methods for planetary vital signs

Ripple et al. (2020) compiled a set of global time series related to human actions that affect the environment and climate (e.g. fossil fuel consumption) and the associated environmental and climatic responses (e.g. temperature change). We have made a number of updates to this set of variables, which are described below. For completeness, we also describe all relevant methods, variables, and sources in full here, but note that there may be some overlap with Ripple et al. (2020) given the nature of this update.

Although the data used are from sources believed to be reliable, no formal accuracy assessment for these datasets has been made by us and users should proceed with caution. With the exception of climate emergency declarations (see next section), all the “human actions” time series are annual. However, many of the “environmental and climatic responses” time series are subannual (e.g., monthly). In contrast to Ripple et al. (2020), we opted to keep these eight time series at their original (source) frequency rather than resampling to annual frequency.

For each variable, we calculated the following statistics:

1. The number of years with data (e.g., a variable with data from 1960 to 2021 would have 62 years of data)
2. The most recent year with data (can be fractional for subannual frequency variables – for example, 2021.35)
3. The most recent value of the variable (year-to-date average for subannual variables)
4. The most recent change in the variable (between current and preceding year-to-date averages for subannual variables)
5. The rank associated with the most recent value (#3) based on the entire time series. For example, a rank of 2 means the variable is at its second highest level ever (second highest year-to-date average for subannual variables).

While we only plotted data between 2000 and the present (2021), we included data from before 2000 (if available) when calculating the above statistics.

Models for vital signs

For area burned in the United States and billion-dollar floods in the United States, we fitted Bayesian changepoint models to explore the possibility of abrupt shifts in these time series. Following Fonnesbeck et al. (2017), we treated the number of billion dollar floods in each year as Poisson distributed, with two rate parameters—one before the breakpoint and another after the breakpoint. We treated the breakpoint location itself as a latent discrete parameter, with a discrete uniform prior. For the rate parameter priors, we used weakly informative exponential distributions with mean 10 (and variance 100). We used the same approach to model area burned, except we treated the data as following exponential distributions, rather than Poisson distributions.

We marginalized out the latent discrete breakpoint parameters and fit the models using the Stan probabilistic programming language (Carpenter et al. 2017). We based inference on 4,000 MCMC posterior samples (from 4 chains with 1,000 burnin samples discarded). It is important to note that this analysis was intended as a simple and preliminary assessment of possible abrupt shifts in certain climate-related disaster variables. To make rigorous conclusions, further research is needed. For example, followup work could consider more flexible probability distributions, account for possible temporal autocorrelation, or incorporate climate-related predictor variables

For the plots of the other “environmental and climatic responses” variables with high variance, we included smooth trend lines calculated using locally estimated scatterplot smoothing. We fit the trend lines in R using the ‘loess’ function with default settings (degree 2, span 0.75) (R Core Team 2018).

Indicators of climate-related human activities (Figure 2)

Below, we list sources and provide brief descriptions of indicators used in our analysis. Full methods for each indicator are available at the provided sources.

Human population (Figure 2a)

We used the Food and Agriculture Organization Corporate Statistical Database (FAOSTAT) as our source of human population data (FAOSTAT 2022). For human population estimates, the source data used by FAOSTAT are derived from national population censuses. For 2019 through 2022, these estimates are classified as "year projections."

Total fertility rate (Figure 2b)

We obtained this variable from the World Bank (The World Bank 2022a). The full variable name is "Fertility rate, total (births per woman)" and the World Bank variables ID is SP.DYN.TFRT.IN. This variable was derived using data from multiple sources, including the United Nations Population Division. The full list of original sources is available at The World Bank (2022a). Total fertility rate is defined as "the number of children that would be born to a woman if she were to live to the end of her childbearing years and bear children in accordance with age-specific fertility rates of the specified year" (The World Bank 2022a).

Ruminant livestock population (Figure 2c)

We used the Food and Agriculture Organization Corporate Statistical Database (FAOSTAT) as our source of ruminant livestock population data (FAOSTAT 2022). We considered ruminants to be members of the following groups: cattle, buffaloes, sheep, and goats. For livestock estimates, the primary data sources are national statistics obtained using questionnaires or collected from countries' websites or reports. When national livestock statistics were unavailable, they were estimated by FAOSTAT using imputation (FAOSTAT 2022).

Per capita meat production (Figure 2d)

We used total meat production data from FAOSTAT along with FAOSTAT human population size estimates (figure 2a) to estimate per capita meat production (FAOSTAT 2022). The meat production estimates are for the "Meat, Total" item under the "Crops and livestock products" domain (FAOSTAT 2022).

World gross domestic product (Figure 2e)

We obtained this variable from the World Bank (2022b) for the years 1960 to 2021. The full variable name is "GDP (constant 2015 US$)" and the World Bank variable ID is

NY.GDP.MKTP.KD. This variable was derived from multiple sources such as World Bank national accounts. For details, including limitations and exceptions, see The World Bank (2022b). Gross domestic product (at purchaser's prices) is defined as "the sum of gross value added by all resident producers in the economy plus any product taxes and minus any subsidies not included in the value of the products" (The World Bank 2022b).

We calculated a projection for 2022 gross domestic product (GDP) using the April 2022 edition of the International Monetary Fund's World Economic Outlook Database (IMF 2022). We first obtained the year 2022 percentage change estimate based on the variable "Gross domestic product, constant prices" in units "Percent change" (IMF 2022). We then used this percentage change estimate to predict total GDP (as measured by the World Bank in constant 2015 US dollars) in 2022. Because IMF projections and World Bank and World Economic Outlook GDP estimates likely differ in methodology, this 2022 estimate should only be considered an approximation.

Global tree cover loss (Figure 2f)

We obtained data on annual global tree cover loss from Global Forest Watch (Hansen et al. 2013). These data express loss globally in million hectares (Mha) and were derived from remotely-sensed forest change maps. It should be noted that loss is general and not linked to a specific type of deforestation. So, it includes wildlife, conversion to agriculture, disease, etc. Additionally, tree cover loss does not take tree cover gain into account. Thus, net forest loss may be lower than the reported numbers.

Some of the apparent variation in loss rates may be due to non-forest factors such as changes in the modeling algorithm, satellite data quality, and satellite data variability (Global Forest Watch 2022). Thus, trends in tree cover loss rates should be interpreted with this limitation in mind.

Brazilian Amazon forest loss (Figure 2g)

We obtained annual Brazilian Amazon forest loss estimates from Butler (2022). Brazil contains about 60% of the Amazon rainforest. We used annual deforestation estimates rather than monthly ones because of high month-to-month variability. Due to cloud cover issues, each annual estimate is for the period August 1 to July 31. For example, the 2021 estimate is for deforestation occurring between August 1, 2020 and July 31, 2021.

The original source of these data is PRODES — the annual deforestation monitoring system of Brazil's National Institute for Space Research (INPE). PRODES deforestation estimates are based on remotely sensed Landsat-type data.

Energy consumption (Figure 2h)

We used the British Petroleum Company's 2022 Statistical Review of World Energy as our primary source of data on energy consumption (British Petroleum Company 2022). For energy consumption, we used the following time series: coal, oil, natural gas, solar, and wind. We grouped solar and wind together into a single category. Coal consumption data are only for commercial solid fuels. In each case, the units of energy consumption are exajoules (per year). Other sources of low carbon energy such as hydropower and nuclear power are shown in figure S3.

Air transport (Figure 2i)

We obtained estimates from the World Bank (The World Bank 2022c). The full variable name is "Air transport, passengers carried." The corresponding World Bank variable ID is IS.AIR.PSGR. This variable was derived from multiple sources, including the International Civil Aviation Organization. The full list of sources is available at The World Bank (2022c). Air transport includes both domestic and international travelers.

Divestment (Figure 2j)

Data on "total assets under management committed to fossil fuel divestment" were obtained from the "Invest Divest 2021" report (DivestInvest 2021). They cover institutional divestment by 1,485 organizations. The most commonly represented institutions were faith-based organizations, educational institutions, philanthropic foundations, governments, and pension funds (DivestInvest 2021). The original source of these data is the Global Divestment Commitments Database, which is "currently managed by Stand.earth in partnership with 350.org" (DivestInvest 2021).

There are several important methodological details for these data:

1. This divestment variable reflects cumulative institutional investment by year in terms of total assets under management (AUM). Thus, it does not represent actual amounts of divestment from fossil fuel companies.
2. Fossil divestment commitments vary in terms of reach and impact. For example, some commitments may only apply to tar sands or thermal coal.
3. Estimates are based on announced fossil fuel divestment commitments.
4. Although the Global Divestment Commitments Database is reported to be the most comprehensive dataset on divestment commitments (DivestInvest 2021), it does not necessarily include all commitments.

For further details and caveats, see the "Methodology" section of the Invest Divest 2021 report (DivestInvest 2021).

Note that more sophisticated metrics are needed to determine which companies should be subject to divestment (Mormann 2020).

CO_2 emissions (Figure 2k)

We used the British Petroleum Company's 2022 Statistical Review of World Energy as our source of data on CO_2 emissions (British Petroleum Company 2022). Specifically, we used the variable "Carbon Dioxide Equivalent Emissions from Energy, Process Emissions, Methane, and Flaring," which is defined as "the sum of carbon dioxide emissions from energy, carbon dioxide emissions from flaring, methane emissions in carbon dioxide equivalent and carbon dioxide emissions from industrial processes" (British Petroleum Company 2022).

Per capita CO_2 emissions (Figure 2l)

We converted total CO_2 emissions (figure 2k) to per capita CO_2 emissions using FAOSTAT human population size estimates (figure 2a).

Greenhouse gas emissions covered by carbon pricing (Figure 2m)

The data on percentage of greenhouse gas emissions covered by carbon pricing schemes are taken directly from World Bank Group (2021). When multiple schemes covered the same emissions, the emissions were associated with the earliest of the schemes. The data were accessed using the Carbon Pricing Dashboard. They were last updated on April 1, 2021.

Carbon price and share of greenhouse gas emissions covered by carbon pricing (Figure 2n)

These data were derived from World Bank Group (2021). To estimate the global carbon price, we used the average of the individual scheme prices weighted by the percentage of greenhouse gas emissions covered by each scheme. When multiple schemes covered the same emissions, the emissions were associated with the earliest of the schemes. The data were accessed using the Carbon Pricing Dashboard. They were last updated on April 1, 2022.

Fossil fuel subsidies (Figure 2o)

We obtained data on fossil fuel subsidies between 2010 and 2020 using the International Energy Agency subsidies database (IEA 2022). Fossil fuel consumption subsidies are global totals in 2020 billion US dollars. They cover oil, electricity, natural gas, and coal.

Subsidy values are estimated using the price-gap approach, which involves comparing "average end-user prices paid by consumers with reference prices that correspond to the full cost of supply" (IEA 2022). The subsidy amount is equal to the product of this price gap and the amount consumed (IEA 2022).

Climate emergency declarations (Figure 2p)

We obtained data on climate emergency declarations from the International Climate Emergency Forum (ICEF) "Governments emergency declaration spreadsheet" (Climate Emergency Declaration 2022). These data track governments that have either declared or recognized a climate emergency. The first declaration in the dataset occurred on December 5, 2016. We converted these data to annual totals by considering only cumulative total declarations at the end of each year. For example, the total number of declarations by 2018 corresponds to the number of declarations made prior to December 31, 2018 (including those made in preceding years).

In the manuscript text, we present the number of countries in which one or more jurisdictions have declared a climate emergency. We obtained this information from the International Climate Emergency Forum (ICEF) "Governments emergency declaration spreadsheet" (Climate Emergency Declaration 2022).

Indicators of climate-related responses (Figure 3)

Atmospheric CO_2 (Figure 3a)

We obtained globally averaged monthly estimates of atmospheric CO_2 concentration from NOAA's Global Monitoring Laboratory (Dlugokencky and Tans 2022). Specifically, we used the dataset "Globally averaged marine surface monthly mean data." Note that data for the most recent year are subject to change; potential changes are typically minor. Beginning on February 10, 2021, these CO_2 data are on the WMO X2019 scale. See Global Monitoring Laboratory (2021) for details on the difficulty in attributing a change in atmospheric CO_2 concentration to COVID-19.

Atmospheric methane (Figure 3b)

We obtained globally-averaged monthly estimates of atmospheric methane (CH_4) concentration from NOAA (Ed Dlugokencky, NOAA/ESRL 2022). We used the "Globally averaged marine surface monthly mean data" dataset. These data are derived from measurements made at a global network of sampling sites that were smoothed across time and plotted versus latitude (Dlugokencky et al. 1994, Masarie and Tans 1995). The data are reported as a "dry air mole fraction" (Ed Dlugokencky, NOAA/ESRL 2022).

Atmospheric nitrous oxide (Figure 3c)

We obtained data on nitrous oxide (N_2O) concentration from the NOAA/ESRL Global Monitoring Laboratory ("Globally averaged marine surface monthly mean data") (Ed Dlugokencky, NOAA/GML 2022). These global monthly mean estimates are measured in parts per billion and are derived by smoothing data collected from a global network of airs sampling sites (Dlugokencky et al. 1994, Masarie and Tans 1995).

Surface temperature anomaly (change) (Figure 3d)

We obtained global monthly mean surface temperature anomaly data from the NASA GISS Surface Temperature Analysis (GISTEMP v4) dataset (GISTEMP Team 2022). We used the "Combined Land-Surface Air and Sea-Surface Water Temperature Anomalies (Land-Ocean Temperature Index, L-OTI)" "Global-mean monthly, seasonal, and annual means" variable. These temperature anomaly/change estimates combine land and ocean surface temperatures. The baseline period used for setting zero is the 1951-1980 mean.

Minimum Arctic sea ice (Figures 3e)

We obtained minimum Arctic sea ice estimates from Wiese (2019) and NSIDC/NASA (2022). They are derived from satellite observations. For each year, the data indicate the average Arctic sea ice extent for the month of September, which is when the annual minimum occurs.

According to NSIDC/NASA (2022), "Arctic sea ice reaches its minimum each September. September Arctic sea ice is now declining at a rate of 13.1 percent per decade, relative to the 1981 to 2010 average." For plotting purposes, we associated each observation with September 15 (the approximate midpoint of the month).

Greenland ice mass (Figure 3f)

We obtained total land ice mass change measurements for Greenland from Wiese (2019) and NSIDC/NASA (2022). These data show changes in ice sheet mass (in Gt) since April 2002. They come from NASA's GRACE satellites (GRACE and GRACE-FO JPL RL06Mv2 Mascon Solution). The data are in the form of anomalies relative to April 2002. The measurement frequency is roughly monthly. The gap in the data between June 10, 2017 and June 14, 2018 corresponds to the time between missions, and should be kept in mind when interpreting the year-to-date means that we present. For more details on these data, see Watkins et al. (2015).

Antarctica ice mass (Figure 3g)

We obtained total land ice mass change measurements for Antarctica from Wiese (2019). These data show the changes in ice sheet mass (in Gt) since April 2002. They come from NASA's GRACE satellites (GRACE and GRACE-FO JPL RL06Mv2 Mascon Solution). The measurement frequency is roughly monthly. The gap in the data between June 10, 2017 and June 14, 2018 corresponds to the time between missions, and should be kept in mind when interpreting the year-to-date means that we present. For more details on these data, see Watkins et al. (2015).

Cumulative glacier thickness change (Figure 3h)

We obtained cumulative glacier mass balance data from the World Glacier Monitoring Service (WGMS 2022). These data were derived from a database with information about changes in mass, volume, etc. of individual glaciers over time. They are based on averaging over a global set of reference glaciers and are measured relative to 1970.

The units of these data are meters of water equivalent. According to the World Glacier Monitoring Service, "A value of -1.0 [meter of water equivalent] per year is representing a mass loss of 1,000 kg per square meter of ice cover or an annual glacier-wide ice thickness loss of about 1.1 m per year, as the density of ice is only 0.9 times the density of water" (WGMS 2022).

For plotting, we associated each value with the midpoint of the corresponding year.

Ocean heat content (Figure 3i)

We obtained yearly (not pentadal) ocean heat content time series data from NOAA's National Centers for Environmental Information (NCEI) (NOAA 2022a). These data are in units of 10^{22}

joules and cover the depth range 0-2000 m. The reference period is 1955-2006 (Levitus et al. 2012).

For plotting, we associated each value with the midpoint of the corresponding year (as in the dataset).

Ocean acidity (Figure 3j)

As a proxy for global ocean acidity, we used a time series of seawater pH from the Hawaii Ocean Time-series surface CO2 system data product (HOT 2022). This data product was adapted from Dore et al. (2009). The data were collected at Station ALOHA (22°45'N, 158°00'W). We used the variable "pHmeas_insitu," which is described as the "mean measured seawater pH, adjusted to in situ temperature, on the total scale" (HOT 2022).

Sea level change (Figure 3k)

We obtained data on global mean sea level from GSFC (2021). The variable we used was "GMSL (Global Isostatic Adjustment (GIA) not applied) variation (mm) with respect to 20-year TOPEX/Jason collinear mean reference." According to the dataset description, the "TOPEX/Jason 20 year collinear mean reference is derived from cycles 121 to 858, years 1996-2016" (GSFC 2021). For details, see Beckley et al. (2010) and Beckley et al. (2017).

It should be noted that temperature increase and the warming of the entire ocean is a major contributor to sea-level rise (WCRP Global Sea Level Budget Group 2018).

Total area burned by wildfires in the United States (Figure 3l)

These data come from the National Interagency Coordination Center at The National Interagency Fire Center (National Interagency Coordination Center 2022) and include Alaska and Hawaii. The total for 2004 does not include state lands within North Carolina.

Although wildfire risk depends on many factors including forest management, climate change is likely a significant contributor in the United States (An et al. 2015) and globally (Jolly et al. 2015).

As with global tree cover loss due to fires (figure 3m), this dataset does not distinguish between natural and human-ignited fires.

Global tree cover loss due to fires (Figure 3m)

We obtained global estimates of tree cover loss due to fires from Tyukavina et al. (2022). Tree cover refers to vegetation with height 5 m or greater. These estimates exclude the burning of felled trees, but include both natural and human-ignited fires (Tyukavina et al. 2022).

These data were downloaded using the Global Forest Watch platform (World Resources Institute 2022).

Billion-dollar floods in the United States (Figure 3n)

We obtained data on the frequency of billion-dollar floods in the United States from NOAA (2022b). This dataset covers the number of floods per year (since 1980) with at least 1 billion USD in damages. All damage estimates were CPI-adjusted to 2022 (NOAA 2022b). See Smith (2022) for details.

Climate change is likely associated with increasing flood risk in many parts of the world, although estimates may be highly uncertain (Hirabayashi et al. 2013, Alfieri et al. 2017). Because the data we present relate to economic damages, an increasing trend may be partly due to rising vulnerability, exposure, and GDP (Cardona et al. 2012, Lavell et al. 2012).

Extremely hot days relative to 1961-1990 (Figure 3o)

We used the "TX90p" temperature metric to assess the frequency of extremely hot days (Donat et al. 2013). This variable is derived from the GHCNDEX dataset and indicates the proportion of days where the maximum temperature exceeds the 90th percentile for the baseline period 1961-1990. Thus, it should remain around 10% in the absence of an overall temperature trend. To obtain a single global time series, the gridded spatio-temporal time series were averaged across Earth's surface (from -84 to 84 latitude). For details, see Zhang et al. (2005) and Donat et al. (2013).

Note that climate change has been linked to increases in both the frequency and intensity of extreme heat events (Luber and McGeehin 2008).

Dengue virus vector capacity (Figure 3p)

Watts et al. (2019) presented estimates of global vectorial capacity for two dengue virus vectors: the mosquito species *Aedes aegypti* and *Aedes albopictus*. The vectorial capacities associated with these species are measures of their propensity to transmit the dengue virus (Liu-Helmersson et al. 2014). These data cover the timespan 1950 to 2017 and are expressed in terms of % change relative to ca. 1950 (Watts et al. 2019). We estimated overall vectorial capacity change by averaging these time series together. Since these vectors have different baseline capacities, the average that we present is only intended as a rough indicator of overall capacity.

Supplemental References

Alfieri L, Bisselink B, Dottori F, Naumann G, de Roo A, Salamon P, Wyser K, Feyen L. 2017. Global projections of river flood risk in a warmer world. Earth's Future 5: 171–182.

An H, Gan J, Cho SJ. 2015. Assessing climate change impacts on wildfire risk in the United States. Forests 6: 3197–3211.

Beckley B, Zelensky N, Holmes S, Lemoine F, Ray R, Mitchum G, Desai S, Brown S. 2010. Assessment of the Jason-2 extension to the TOPEX/Poseidon, Jason-1 sea-surface height time series for global mean sea level monitoring. Marine Geodesy 33: 447–471.

Beckley BD, Callahan PS, Hancock III D, Mitchum G, Ray R. 2017. On the "Cal-Mode" correction to TOPEX satellite altimetry and its effect on the global mean sea level time series. Journal of Geophysical Research: Oceans 122: 8371–8384.

Boulton CA, Lenton TM, Boers N. 2022. Pronounced loss of Amazon rainforest resilience since the early 2000s. Nature Climate Change 12: 271–278.

British Petroleum Company. 2022. BP statistical review of world energy. British Petroleum Company.

Buchner B, Naran B, Fernandes P de A, Padmanabhi R, Rosane P, Solomon M, Stout S, Wakaba G, Zhu Y, Meattle C, Guzmán S, Strinati C. 2021. Global Landscape of Climate Finance 2021.

Butler RA. 2022. Amazon deforestation on pace to roughly match last year's rate of loss. Mongabay. (17 August 2022; https://news.mongabay.com/2022/08/amazon-deforestation-on-pace-for-near-record-year/).

Cardona OD, Van Aalst MK, Birkmann J, Fordham M, Mc Gregor G, Rosa P, Pulwarty RS, Schipper ELF, Sinh BT, Décamps H, others. 2012. Determinants of risk: exposure and vulnerability. Pages 65–108 in. Managing the risks of extreme events and disasters to advance climate change adaptation: special report of the intergovernmental panel on climate change. Cambridge University Press.

Carpenter B, Gelman A, Hoffman MD, Lee D, Goodrich B, Betancourt M, Brubaker M, Guo J, Li P, Riddell A. 2017. Stan: A probabilistic programming language. Journal of statistical software 76.

Climate Emergency Declaration. 2022. Climate Emergency Declaration. Climate emergency declarations in 2,094 jurisdictions and local governments cover 1 billion citizens. (1 May 2022; https://climateemergencydeclaration.org/climate-emergency-declarations-cover-15-million-citizens/).

DivestInvest. 2021. Invest Divest 2021. (29 September 2022; https://www.divestinvest.org/invest-divest-2021/).

Dlugokencky E, Steele L, Lang P, Masarie K. 1994. The growth rate and distribution of atmospheric methane. Journal of Geophysical Research: Atmospheres 99: 17021–17043.

Dlugokencky E, Tans P. 2022. NOAA/GML. Trends in Atmospheric Carbon Dioxide. NOAA/GML. (3 May 2022; https://www.esrl.noaa.gov/gmd/ccgg/trends/).

Donat MG, Alexander LV, Yang H, Durre I, Vose R, Caesar J. 2013. Global land-based datasets for monitoring climatic extremes. Bulletin of the American Meteorological Society 94: 997–1006.

Ed Dlugokencky, NOAA/ESRL. 2022. Trends in Atmospheric Methane. Trends in Atmospheric Methane. (3 May 2022; https://www.esrl.noaa.gov/gmd/ccgg/trends_ch4/).

Ed Dlugokencky, NOAA/GML. 2022. Trends in Atmospheric Nitrous Oxide. Trends in Atmospheric Nitrous Oxide. (3 May 2022; https://www.esrl.noaa.gov/gmd/ccgg/trends_n2o/).

FAOSTAT. 2022. FAOSTAT Database on Agriculture. FAOSTAT Database on Agriculture. (26 April 2022; http://faostat.fao.org/).

Fonnesbeck CJ, Patil A, Huard D, Salvatier J. 2017. PyMC Documentation.

Friedlingstein P, Jones MW, O'Sullivan M, Andrew RM, Bakker DCE, Hauck J, Le Quéré C, Peters GP, Peters W, Pongratz J, Sitch S, Canadell JG, Ciais P, Jackson RB, Alin SR, Anthoni P, Bates NR, Becker M, Bellouin N, Bopp L, Chau TTT, Chevallier F, Chini LP, Cronin M, Currie KI, Decharme B, Djeutchouang LM, Dou X, Evans W, Feely RA, Feng L, Gasser T, Gilfillan D, Gkritzalis T, Grassi G, Gregor L, Gruber N, Gürses Ö, Harris I, Houghton RA, Hurtt GC, Iida Y, Ilyina T, Luijkx IT, Jain A, Jones SD, Kato E, Kennedy D, Klein Goldewijk K, Knauer J, Korsbakken JI, Körtzinger A, Landschützer P, Lauvset SK, Lefèvre N, Lienert S, Liu J, Marland G, McGuire PC, Melton JR, Munro DR, Nabel JEMS, Nakaoka S-I, Niwa Y, Ono T, Pierrot D, Poulter B, Rehder G, Resplandy L, Robertson E, Rödenbeck C, Rosan TM, Schwinger J, Schwingshackl C, Séférian R, Sutton AJ, Sweeney C, Tanhua T, Tans PP, Tian H, Tilbrook B, Tubiello F, van der Werf GR, Vuichard N, Wada C, Wanninkhof R, Watson AJ, Willis D, Wiltshire AJ, Yuan W, Yue C, Yue X, Zaehle S, Zeng J. 2022. Global Carbon Budget 2021. Earth System Science Data 14: 1917–2005.

Ghebrezgabher MG, Yang T, Yang X. 2016. Long-term trend of climate change and drought assessment in the Horn of Africa. Advances in Meteorology 2016.

GISTEMP Team. 2022. GISS Surface Temperature Analysis (GISTEMP), version 4. NASA Goddard Institute for Space Studies. (3 May 2022; https://data.giss.nasa.gov/gistemp/).

Global Forest Watch. 2022. Assessing Trends in Tree Cover Loss Over 20 Years of Data. (17 August 2022; https://www.globalforestwatch.org/blog/data-and-research/tree-cover-loss-satellite-data-trend-analysis/).

Global Monitoring Laboratory. 2021. Can we see a change in the CO2 record because of COVID-19? Can we see a change in the CO2 record because of COVID-19? (30 April 2021; https://www.esrl.noaa.gov/gmd/ccgg/covid2.html).

GSFC. 2021. Global Mean Sea Level Trend from Integrated Multi-Mission Ocean Altimeters TOPEX/Poseidon, Jason-1, OSTM/Jason-2, and Jason-3 Version 5.1 Ver. 5.1.

Hansen MC, Potapov PV, Moore R, Hancher M, Turubanova SA, Tyukavina A, Thau D, Stehman SV, Goetz SJ, Loveland TR, Kommareddy A, Egorov A, Chini L, Justice CO, Townshend JRG. 2013. High-Resolution Global Maps of 21st-Century Forest Cover Change. Science 342: 850-853. Data available on-line from:http://earthenginepartners.appspot.com/science-2013-global-forest. Accessed through Global Forest Watch on 6/29/22. www.globalforestwatch.org.

Hausfather Z. 2022. Global CO2 emissions have been flat for a decade, new data reveals. Carbon Brief. (15 August 2022; https://www.carbonbrief.org/global-co2-emissions-have-been-flat-for-a-decade-new-data-reveals/).

Hirabayashi Y, Mahendran R, Koirala S, Konoshima L, Yamazaki D, Watanabe S, Kim H, Kanae S. 2013. Global flood risk under climate change. Nature Climate Change 3: 816–821.

HOT. 2022. Hawaii Ocean Time-series (HOT). Hawaii Ocean Time-series (HOT). (4 May 2022; https://hahana.soest.hawaii.edu/hot/hotco2/hotco2.html).

IEA. 2022. Energy subsidies: Tracking the impact of fossil-fuel subsidies. International Energy Agency.

IMF. 2022. World Economic Outlook Database: April 2022 Edition. International Monetary Fund.

IPCC. 2018. Global Warming of 1.5° C: An IPCC Special Report on the Impacts of Global Warming of 1.5° C Above Pre-industrial Levels and Related Global Greenhouse Gas Emission Pathways, in the Context of Strengthening the Global Response to the Threat of Climate Change, Sustainable Development, and Efforts to Eradicate Poverty. Intergovernmental Panel on Climate Change.

Jolly WM, Cochrane MA, Freeborn PH, Holden ZA, Brown TJ, Williamson GJ, Bowman DM. 2015. Climate-induced variations in global wildfire danger from 1979 to 2013. Nature communications 6: 1–11.

Lavell A, Oppenheimer M, Diop C, Hess J, Lempert R, Li J, Muir-Wood R, Myeong S, Moser S, Takeuchi K, others. 2012. Climate change: new dimensions in disaster risk, exposure, vulnerability, and resilience. Pages 25–64 in. Managing the risks of extreme events and disasters to advance climate change adaptation: Special report of the intergovernmental panel on climate change. Cambridge University Press.

Lenton TM, Rockström J, Gaffney O, Rahmstorf S, Richardson K, Steffen W, Schellnhuber HJ. 2019. Climate tipping points—too risky to bet against. Nature 575: 592–595.

Liu-Helmersson J, Stenlund H, Wilder-Smith A, Rocklöv J. 2014. Vectorial capacity of Aedes aegypti: effects of temperature and implications for global dengue epidemic potential. PloS one 9: e89783.

Luber G, McGeehin M. 2008. Climate change and extreme heat events. American journal of preventive medicine 35: 429–435.

Masarie KA, Tans PP. 1995. Extension and integration of atmospheric carbon dioxide data into a globally consistent measurement record. Journal of Geophysical Research: Atmospheres 100: 11593–11610.

Mormann F. 2020. Why the divestment movement is missing the mark. Nature Climate Change 10: 1067–1068.

Mukherjee S, Mishra A, Trenberth KE. 2018. Climate change and drought: a perspective on drought indices. Current Climate Change Reports 4: 145–163.

National Interagency Coordination Center. 2022. National Interagency Fire Center. National Interagency Fire Center. (3 May 2022; https://www.nifc.gov/fireInfo/fireInfo_stats_totalFires.html).

NOAA. 2022a. National Centers for Environmental Information: Global Ocean Heat and Salt Content. Global Ocean Heat and Salt Content. (3 May 2022; https://www.nodc.noaa.gov/OC5/3M_HEAT_CONTENT/).

NOAA. 2022b. National Centers for Environmental Information (NCEI) U.S. Billion-Dollar Weather and Climate Disasters. (https://www.ncei.noaa.gov/access/monitoring/billions/).

NSIDC/NASA. 2022. Global Climate Change: Vital Signs of the Planet. Arctic Sea Ice Minimum. (3 May 2022; https://climate.nasa.gov/).

Persson L, Carney Almroth BM, Collins CD, Cornell S, de Wit CA, Diamond ML, Fantke P, Hassellöv M, MacLeod M, Ryberg MW, others. 2022. Outside the safe operating space of the planetary boundary for novel entities. Environmental science & technology 56: 1510–1521.

Ripple WJ, Wolf C, Newsome TM, Barnard P, Moomaw WR. 2020. World scientists' warning of a climate emergency. BioScience 70: 8–12.

Rockström J, Beringer T, Hole D, Griscom B, Mascia MB, Folke C, Creutzig F. 2021. We need biosphere stewardship that protects carbon sinks and builds resilience. Proceedings of the National Academy of Sciences 118: e2115218118.

Rousi E, Kornhuber K, Beobide-Arsuaga G, Luo F, Coumou D. 2022. Accelerated western European heatwave trends linked to more-persistent double jets over Eurasia. Nature communications 13: 1–11.

Schuur EA, McGuire AD, Schädel C, Grosse G, Harden J, Hayes DJ, Hugelius G, Koven CD, Kuhry P, Lawrence DM, others. 2015. Climate change and the permafrost carbon feedback. Nature 520: 171–179.

Smith AB. 2022. 2021 U.S. billion-dollar weather and climate disasters in historical context. (4 May 2022; https://www.climate.gov/news-features/blogs/beyond-data/2021-us-billion-dollar-weather-and-climate-disasters-historical).

Steffen W, Richardson K, Rockström J, Cornell SE, Fetzer I, Bennett EM, Biggs R, Carpenter SR, De Vries W, De Wit CA, others. 2015. Planetary boundaries: Guiding human development on a changing planet. science 347: 1259855.

Stendel M, Francis J, White R, Williams PD, Woollings T. 2021. The jet stream and climate change. Pages 327–357 in. Climate Change. Elsevier.

Stott PA, Allen M, Christidis N, Dole RM, Hoerling M, Huntingford C, Pall P, Perlwitz J, Stone D. 2013. Attribution of weather and climate-related events. Pages 307–337 in. Climate science for serving society. Springer.

Strauss BH, Orton PM, Bittermann K, Buchanan MK, Gilford DM, Kopp RE, Kulp S, Massey C, de Moel H, Vinogradov S. 2021. Economic damages from Hurricane Sandy attributable to sea level rise caused by anthropogenic climate change. Nature communications 12: 1–9.

The World Bank. 2022a. Fertility rate, total (births per woman). World Bank.

The World Bank. 2022b. GDP (constant 2015 US$). World Bank.

The World Bank. 2022c. Air transport, passengers carried. World Bank.

Trenberth KE, Fasullo JT, Shepherd TG. 2015. Attribution of climate extreme events. Nature Climate Change 5: 725–730.

Tyukavina A, Potapov P, Hansen MC, Pickens AH, Stehman SV, Turubanova S, Parker D, Zalles V, Lima A, Kommareddy I, others. 2022. Global Trends of Forest Loss Due to Fire From 2001 to 2019. Frontiers in Remote Sensing 3: 825190.

Wackernagel M, Schulz NB, Deumling D, Linares AC, Jenkins M, Kapos V, Monfreda C, Loh J, Myers N, Norgaard R, others. 2002. Tracking the ecological overshoot of the human economy. Proceedings of the national Academy of Sciences 99: 9266–9271.

Wang-Erlandsson L, Tobian A, van der Ent RJ, Fetzer I, te Wierik S, Porkka M, Staal A, Jaramillo F, Dahlmann H, Singh C, others. 2022. A planetary boundary for green water. Nature Reviews Earth & Environment 1–13.

Watkins MM, Wiese DN, Yuan D-N, Boening C, Landerer FW. 2015. Improved methods for observing Earth's time variable mass distribution with GRACE using spherical cap mascons. Journal of Geophysical Research: Solid Earth 120: 2648–2671.

Watts N, Amann M, Arnell N, Ayeb-Karlsson S, Belesova K, Boykoff M, Byass P, Cai W, Campbell-Lendrum D, Capstick S, others. 2019. The 2019 report of The Lancet Countdown on health and climate change: ensuring that the health of a child born today is not defined by a changing climate. The Lancet 394: 1836–1878.

WCRP Global Sea Level Budget Group. 2018. Global sea-level budget 1993–present. Earth System Science Data 10: 1551–1590.

WGMS. 2022. The World Glacier Monitoring Service. (3 May 2022; https://wgms.ch/global-glacier-state/).

Wiese D, Yuan D, Boening C, Landerer F, Watkins M. 2019. JPL GRACE and GRACE-FO Mascon Ocean, Ice, and Hydrology Equivalent Water Height RL06M CRI Filtered Version 2.0, Ver. 2.0. PO.DAAC, CA, USA.

World Bank Group. 2021. State and Trends of Carbon Pricing 2021. World Bank, Washington, DC.

World Resources Institute. 2022. Global Forest Watch. (17 August 2022; https://www.globalforestwatch.org/).

Zhang X, Hegerl G, Zwiers FW, Kenyon J. 2005. Avoiding inhomogeneity in percentile-based indices of temperature extremes. Journal of Climate 18: 1641–1651.